

5. DYNAMICAL THEORY AND ITS APPLICATIONS

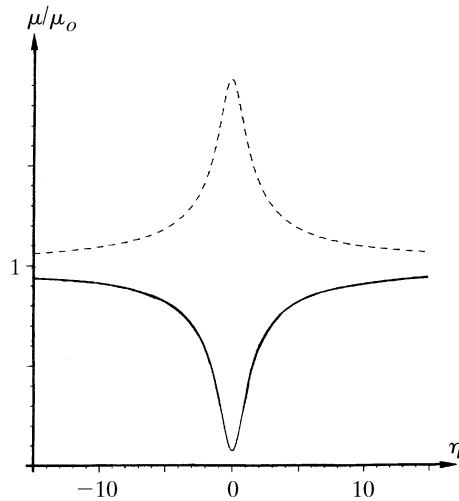


Fig. 5.1.6.1. Variation of the effective absorption with the deviation parameter in the transmission case for the 400 reflection of GaAs using Cu $K\alpha$ radiation. Solid curve: branch 1; broken curve: branch 2.

$$\mu_j = \mu_o \left[1 \mp \frac{|C| |F_{ih}/F_{io}| \cos \varphi}{(\eta_r^2 + 1)^{1/2}} \right].$$

Fig. 5.1.6.1 shows the variations of the effective absorption coefficient μ_j with η_r for wavefields belonging to branches 1 and 2 in the case of the 400 reflection of GaAs with Cu $K\alpha$ radiation. It can be seen that for $\eta_r = 0$ the absorption coefficient for branch 1 becomes significantly smaller than the normal absorption coefficient, μ_o . The minimum absorption coefficient, $\mu_o(1 - |CF_{ih}/F_{io}| \cos \varphi)$, depends on the nature of the reflection through the structure factor and on the temperature through the Debye–Waller factor included in F_{ih} [equation (5.1.2.10b)] (Ohtsuki, 1964, 1965). For instance, in diamond-type structures, it is smaller for reflections with even indices than for reflections with odd indices. The influence of temperature is very important when $|F_{ih}/F_{io}|$ is close to one; for example, for germanium 220 and Mo $K\alpha$ radiation, the minimum absorption coefficient at 5 K is reduced to about 1% of its normal value, μ_o (Ludewig, 1969).

5.1.6.2. Boundary conditions for the amplitudes at the entrance surface – intensities of the reflected and refracted waves

Let us consider an infinite plane wave incident on a crystal plane surface of infinite lateral extension. As has been shown in Section 5.1.3, two wavefields are excited in the crystal, with tie points P_1 and P_2 , and amplitudes D_{o1}, D_{h1} and D_{o2}, D_{h2} , respectively. Maxwell's boundary conditions (see Section A5.1.1.2 of the Appendix) imply continuity of the tangential component of the electric field and of the normal component of the electric displacement across the boundary. Because the index of refraction is so close to unity, one can assume to a very good approximation that there is continuity of the three components of both the electric field and the electric displacement. As a consequence, it can easily be shown that, *along the entrance surface*, for all components of the electric displacement

$$\begin{aligned} D_o^{(a)} &= D_{o1} + D_{o2} \\ 0 &= D_{h1} + D_{h2}, \end{aligned} \quad (5.1.6.2)$$

where $D_o^{(a)}$ is the amplitude of the incident wave.

Using (5.1.3.11), (5.1.5.2) and (5.1.6.2), it can be shown that the intensities of the four waves are

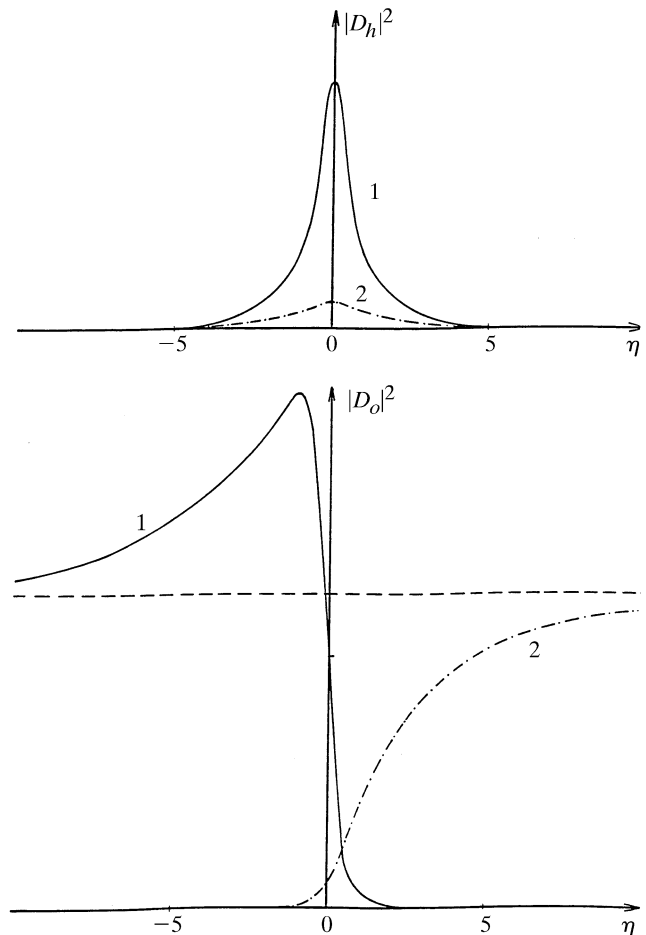


Fig. 5.1.6.2. Variation of the intensities of the reflected and refracted waves in an absorbing crystal for the 220 reflection of Si using Mo $K\alpha$ radiation, $t = 1$ mm ($\mu t = 1.42$). Solid curve: branch 1; dashed curve: branch 2.

$$\begin{aligned} |D_{oj}|^2 &= |D_o^{(a)}|^2 \exp(-\mu_j z / \gamma_o) \left[(1 + \eta_r^2)^{1/2} \mp \eta_r \right]^2 \\ &\quad \times [4(1 + \eta_r^2)]^{-1}, \end{aligned} \quad (5.1.6.3)$$

$$|D_{hj}|^2 = |D_o^{(a)}|^2 \exp(-\mu_j z / \gamma_o) |F_h/F_{\bar{h}}| [4\gamma(1 + \eta_r^2)]^{-1};$$

top sign: $j = 1$; bottom sign: $j = 2$.

Fig. 5.1.6.2 represents the variations of these four intensities with the deviation parameter. Far from the reflection domain, $|D_{h1}|^2$ and $|D_{h2}|^2$ tend toward zero, as is normal, while

$$|D_{o1}|^2 \gg |D_{o2}|^2 \text{ for } \eta_r \Rightarrow -\infty,$$

$$|D_{o1}|^2 \ll |D_{o2}|^2 \text{ for } \eta_r \Rightarrow +\infty.$$

This result shows that the wavefield of highest intensity 'jumps' from one branch of the dispersion surface to the other across the reflection domain. This is an important property of dynamical theory which also holds in the Bragg case and when a wavefield crosses a highly distorted region in a deformed crystal [the so-called *interbranch scattering*; see, for instance, Authier & Balibar (1970) and Authier & Malgrange (1998)].

5.1.6.3. Boundary conditions at the exit surface

5.1.6.3.1. Wavevectors

When a wavefield reaches the exit surface, it breaks up into its two constituent waves. Their wavevectors are obtained by applying

5.1. DYNAMICAL THEORY OF X-RAY DIFFRACTION

again the condition of the continuity of their tangential components along the crystal surface. The extremities, M_j and N_j , of these wavevectors

$$\mathbf{OM}_j = \mathbf{K}_{o_j}^{(d)} \quad \mathbf{HN}_j = \mathbf{K}_{h_j}^{(d)}$$

lie at the intersections of the spheres of radius k centred at O and H , respectively, with the normal \mathbf{n}' to the crystal exit surface drawn from P_j ($j = 1$ and 2) (Fig. 5.1.6.3).

If the crystal is wedge-shaped and the normals \mathbf{n} and \mathbf{n}' to the entrance and exit surfaces are not parallel, the wavevectors of the waves generated by the two wavefields are not parallel. This effect is due to the refraction properties associated with the dispersion surface.

5.1.6.3.2. Amplitudes – Pendellösung

We shall assume from now on that the crystal is plane parallel. Two wavefields arrive at any point of the exit surface. Their constituent waves interfere and generate emerging waves in the refracted and reflected directions (Fig. 5.1.6.4). Their respective

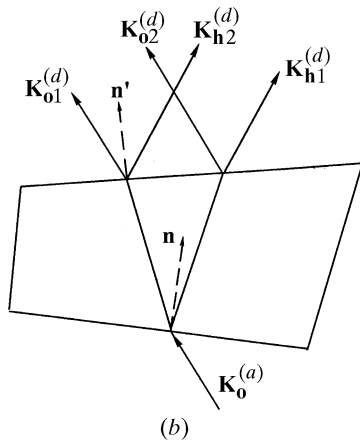
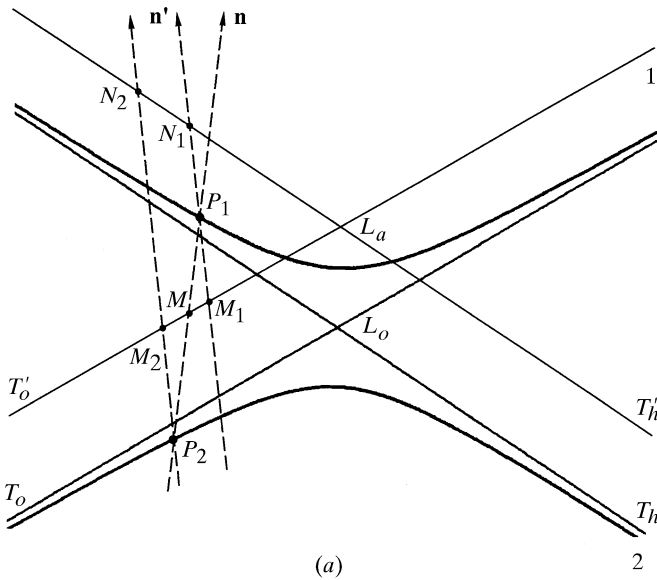


Fig. 5.1.6.3. Boundary condition for the wavevectors at the exit surface. (a) Reciprocal space. The wavevectors of the emerging waves are determined by the intersections M_1 , M_2 , N_1 and N_2 of the normals \mathbf{n}' to the exit surface, drawn from the tie points P_1 and P_2 of the wavefields, with the tangents T_o' and T_h' to the spheres centred at O and H and of radius k , respectively. (b) Direct space.

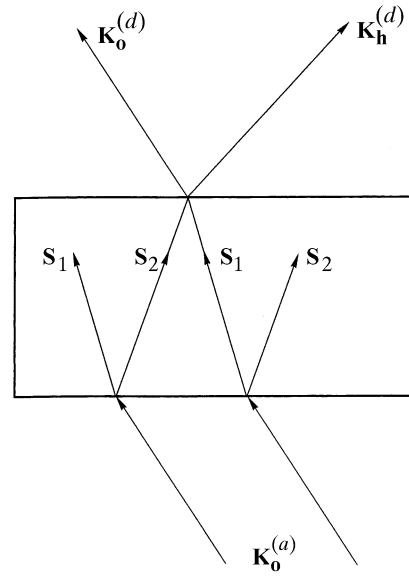


Fig. 5.1.6.4. Decomposition of a wavefield into its two components when it reaches the exit surface. \mathbf{S}_1 and \mathbf{S}_2 are the Poynting vectors of the two wavefields propagating in the crystal belonging to branches 1 and 2 of the dispersion surface, respectively, and interfering at the exit surface.

amplitudes are given by the boundary conditions

$$\begin{aligned} D_o^{(d)} \exp(-2\pi i \mathbf{K}_o^{(d)} \cdot \mathbf{r}) &= D_{o1} \exp(-2\pi i \mathbf{K}_{o1} \cdot \mathbf{r}) \\ &\quad + D_{o2} \exp(-2\pi i \mathbf{K}_{o2} \cdot \mathbf{r}) \\ D_h^{(d)} \exp(-2\pi i \mathbf{K}_h^{(d)} \cdot \mathbf{r}) &= D_{h1} \exp(-2\pi i \mathbf{K}_{h1} \cdot \mathbf{r}) \\ &\quad + D_{h2} \exp(-2\pi i \mathbf{K}_{h2} \cdot \mathbf{r}), \end{aligned} \quad (5.1.6.4)$$

where \mathbf{r} is the position vector of a point on the exit surface, the origin of phases being taken at the entrance surface.

In a plane-parallel crystal, (5.1.6.4) reduces to

$$\begin{aligned} D_o^{(d)} &= D_{o1} \exp(-2\pi i \overline{MP}_1 \cdot t) + D_{o2} \exp(-2\pi i \overline{MP}_2 \cdot t) \\ D_h^{(d)} &= D_{h1} \exp(-2\pi i \overline{MP}_1 \cdot t) + D_{h2} \exp(-2\pi i \overline{MP}_2 \cdot t), \end{aligned}$$

where t is the crystal thickness.

In a *non-absorbing* crystal, the amplitudes squared are of the form

$$|D_o^{(d)}|^2 = |D_{o1}|^2 + |D_{o2}|^2 + 2D_{o1}D_{o2} \cos 2\pi \overline{P_2P_1} t.$$

This expression shows that the intensities of the refracted and reflected beams are oscillating functions of crystal thickness. The period of the oscillations is called the *Pendellösung* distance and is

$$\Lambda = 1/\overline{P_2P_1} = \Lambda_L/(1 + \eta_r^2)^{1/2}.$$

5.1.6.4. Reflecting power

For an *absorbing* crystal, the intensities of the reflected and refracted waves are

$$\begin{aligned} |D_o^{(d)}|^2 &= |D_o^{(a)}|^2 A_\eta \left\{ \cosh(2v + \mu_a t) \right. \\ &\quad \left. + \cos \left[2\pi t \Lambda^{-1} - 2\eta_i (1 + \eta_r^2)^{-1/2} \right] \right\} \\ |D_h^{(d)}|^2 &= |D_o^{(a)}|^2 |F_h/F_h| \gamma^{-1} A_\eta \left[\cosh(\mu_a t) - \cos(2\pi t \Lambda^{-1}) \right], \end{aligned} \quad (5.1.6.5)$$

where